

Structure and bonding of Bi-Sr-Ca-Cu-O crystal by x-ray photoelectron spectroscopy

S. Kohiki,* T. Wada, and S. Kawashima

Central Research Laboratory, Matsushita Electric Industries, Moriguchi, Osaka 570, Japan

H. Takagi and S. Uchida

Engineering Research Institute, Faculty of Engineering, University of Tokyo, Bunkyo-ku, Tokyo 113, Japan

S. Tanaka

International Superconductivity Technology Center, Shinbashi, Minato-ku, Tokyo 105, Japan

(Received 17 June 1988; revised manuscript received 25 July 1988)

X-ray photoelectron spectroscopy was performed on high- T_c superconducting Bi-Sr-Ca-Cu-O single crystals with $T_c \sim 80$ K. The core-level electron spectra of Sr, Ca, and Bi show the possibility of exchanging their lattice sites in the crystal. On the other hand, the core-level electron spectrum of Cu indicates a unique lattice site in the crystal. These features are consistent with the structure model for the crystal with formula unit $\text{Bi}_2(\text{Sr,Ca})_3\text{Cu}_2\text{O}_y$. We can readily determine the distribution of Sr, Ca, and Bi in the cation sites by x-ray photoelectron spectroscopy in contrast to x-ray diffraction and high-resolution transmission electron microscopy.

I. INTRODUCTION

Bednorz and Müller¹ first reported high-temperature ($T_c \sim 30$ K) superconductivity in the La-Ba-Cu-O system. Other workers^{2,3} recorded higher T_c 's (~ 40 K) in the La-Sr-Cu-O systems. Wu *et al.*⁴ discovered 90-K superconductivity in the Y-Ba-Cu-O system. Recently, Maeda, Tanaka, Fukutomi, and Asano⁵ reported that $\text{BiSrCaCu}_2\text{O}_y$ has T_c ranging from 105 to 70 K.

It is of great interest to elucidate the origin of the high- T_c superconductivity. In this experiment we study the electronic state of single-crystal Bi-Sr-Ca-Cu-O ($T_c \sim 80$ K) samples by using x-ray photoelectron spectroscopy, as a step towards understanding the mechanism of high- T_c superconductivity.

The crystal structure of $\text{Bi}_2(\text{Sr,Ca})_3\text{Cu}_2\text{O}_y$ with orthorhombic cell $a \sim 5.4$, $b \sim 27$, and $c \sim 30$ Å has been reported.⁶⁻⁹ The transmission electron microscope observation demonstrated that the material possesses a layered structure like the La-Sr-Cu-O and Y-Ba-Cu-O systems, two Cu-O layers being isolated by Bi-O layers.^{10,11} From the proposed alternating $[\text{Bi-O}]-[(\text{Sr/Ca})\text{-O}]-[\text{Cu-O}]-[(\text{Ca/Sr})\text{-O}]-[\text{Cu-O}]-[(\text{Sr/Ca})\text{-O}]-[\text{Bi-O}]$ -layered structure, we can expect to observe two inequivalent electronic states of Sr and Ca and a different Cu valence from that observed in the Y-Ba-Cu-O system due to lack of the Cu-O chain in the $\text{Bi}_2(\text{Sr,Ca})_3\text{Cu}_2\text{O}_y$ structure.

II. EXPERIMENT

Preparation of the single crystals used in this experiment was described elsewhere in detail.¹² Single crystals were grown in a $\text{Bi}_2\text{O}_3\text{-SrCO}_3\text{-CaCO}_3\text{-CuO}$ solution. Typical dimensions of the crystals were $1.5 \times 0.7 \times 0.1$ mm³. The crystals were 80-K superconductors. In order to avoid the complications arising from the coexistence of two superconducting phases, crystals without any trace of

105-K superconductivity were selected for this work. The crystal possessed the orthorhombic cell with $a = 5.453$, $b = 27.26$, and $c = 31.04$ Å. The c axis is perpendicular to the surface of the thin plate. Transmission electron microscopy revealed that the plate samples possessed a perfect basal cleavage, similar to that of clay minerals. The roughly estimated chemical composition of the crystal, corresponding to $\text{Bi}_2\text{Sr}_{1.4}\text{Ca}_1\text{Cu}_2\text{O}_y$, was determined by electron microprobe analysis (EPMA) without using any reference materials.

A SSI SSX-100 electron spectrometer was used to collect photoelectron spectra with monochromatic Al $K\alpha$ radiation. The linewidth for the Ag $3d_{5/2}$ photopeak was 0.56 eV. The spectrometer was calibrated by utilizing the Au $4f_{7/2}$ electron binding energy (83.93 eV). The probable electron energy uncertainty amounted to 0.05 eV. The normal operating vacuum pressure was less than 5×10^{-9} Torr. Measurement of the electron spectra was carried out after scraping the sample surface with a diamond file to eliminate the effect of adsorbates on the photoelectron spectra and to obtain reliable results. We can perform reliable photoelectron spectroscopy on the freshly scraped surface since the crystals have a perfect basal cleavage and there is no influence of such artifacts.

III. RESULTS AND DISCUSSION

We demonstrate how the distribution of Sr, Ca, and Bi in the cation sites of the single-crystalline Bi-Sr-Ca-Cu-O samples is determined by x-ray photoelectron spectroscopy.

The valence of a cation should be determined by both the distances between the cation and surrounding anions and the coordination numbers of the anions. Bond valence sums for Sr and Ca were calculated following the method of Brown and Altermatt¹³ and are listed in Table I. The values for the cation site A (between the Bi-O and Cu-O

TABLE I. Interatomic distances (Å) and bond valence sums for Sr and Ca.

Cation site	Interatomic distance (Ref. 8)	Bond valence sum	
		Sr	Ca
Site <i>A</i> (between the Bi-O and Cu-O sheets)	2.56(5)×4	1.21	0.81
	2.74(2)×4	0.74	0.50
	2.91(11)×1	0.12	0.08
	
		2.07	1.39
Site <i>B</i> (sandwiched between the adjacent Cu-O sheets)	2.52(5)×8	2.70	1.79

sheets) are 2.07 for Sr and 1.39 for Ca and those for the cation site *B* (sandwiched between the adjacent Cu-O sheets) are 2.70 for Sr and 1.79 for Ca. These values suggest that the cation in the site *B* possesses larger valence than that in the site *A*.

In x-ray photoelectron spectroscopy, a lower (higher) binding-energy photoelectron peak corresponds to the atom possessing less (more) ionic character of the chemical bond. If we can partition the core-level electron spectra of Sr and Ca of the single-crystalline Bi-Sr-Ca-Cu-O samples, the binding-energy difference of the partitioned peaks is in relation to the change of effective electronic charge of Sr/Ca atoms due to the difference in lattice sites in the $\text{Bi}_2(\text{Sr,Ca})_3\text{Cu}_2\text{O}_y$ crystal structure.

The Sr $3d$ and Ca $2p$ spectra of the Bi-Sr-Ca-Cu-O samples are shown in Figs. 1 and 2. Both spectra can be partitioned into two components as shown in the figures. The Sr $3d_{5/2}$ lower binding-energy peak (*L*) is positioned at 131.7 eV and the higher binding-energy peak (*H*) is positioned at 132.9 eV. The Ca $2p_{3/2}$ *L* peak is positioned at 344.7 eV and the *H* peak is positioned at 345.9 eV. The *L* and *H* peaks of the Sr $3d$ and the Ca $2p$ spectra can readily be assigned to the Sr and Ca atoms in site *A* and that in site *B*, respectively. The proposed crystal structure of the

$\text{Bi}_2(\text{Sr,Ca})_3\text{Cu}_2\text{O}_y$, with inequivalent Sr/Ca lattice sites, is consistent with the observed splitting of the Sr and Ca core-level electron peaks for the Bi-Sr-Ca-Cu-O samples.

The difference of divalent ion radius between Sr and Ca is 0.21 Å. However, in spite of such difference, the result indicates that Sr and Ca atoms can occupy both sites in the proposed $\text{Bi}_2(\text{Sr,Ca})_3\text{Cu}_2\text{O}_y$ structure. The intensity ratio of *H* to *L* peaks of the Sr $3d$ and Ca $2p$ spectra is 0.25 and 0.59, respectively. The *H* to *L* ratio expected from the proposed $\text{Bi}_2(\text{Sr,Ca})_3\text{Cu}_2\text{O}_y$ structure is 0.50, if Sr and Ca are randomly distributed among two possible sites so that Sr atoms predominantly occupy lattice site *A* and Ca atoms occupy almost evenly two inequivalent lattice sites *A* and *B* of the Bi-Sr-Ca-Cu-O samples. This suggests that the smaller Ca ion could substitute for the Sr ion. However, the Sr ion would selectively occupy the site *A* and only a little Sr would be located at site *B*. From the results of electron-probe-microanalysis, the rough chemical composition of the crystals can be written as $\text{Bi}_2[\text{Sr}_{(2/3)-(1/12)}\text{Ca}_{(1/3)+(1/12)}]_{(3-0.6)}\text{Cu}_2\text{O}_y$. In the crystals used in this experiment the Sr content is poor and the Ca content is rich in comparison with those of the ideal composition. Such composition variation depleting the Sr content in the Bi-Sr-Ca-Cu-O system has been

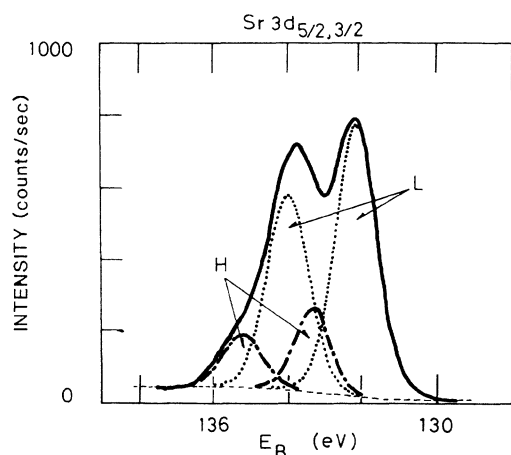


FIG. 1. The Sr $3d$ electron spectrum of the single-crystalline Bi-Sr-Ca-Cu-O samples. The separated peaks have a shape of 100% G and 1.25 eV full width at half maxima. The binding-energy difference between *L* and *H* peaks was 1.2 eV.

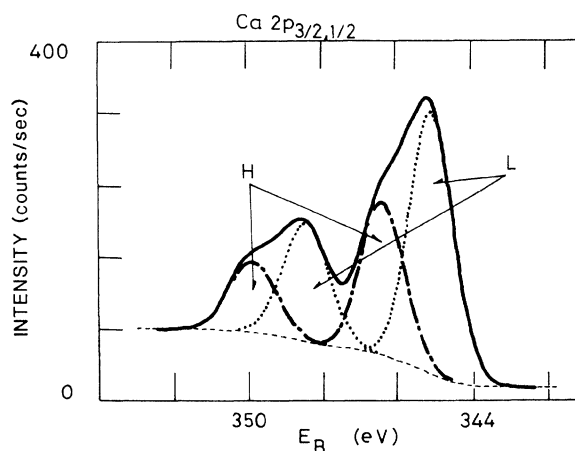


FIG. 2. The Ca $2p$ electron spectrum of the single-crystalline Bi-Sr-Ca-Cu-O samples. The separated peaks have a shape of 100% G and 1.35 eV full width at half maxima. The binding-energy difference between *L* and *H* peaks was 1.2 eV.

TABLE II. Interatomic distances (\AA) and bond valence sums for Bi.

Cation site	Interatomic distance (Ref. 8)	Bond valence sums
Site <i>C</i> (in the Bi-O sheet)	$2.22(7) \times 1$	0.71
	$2.71(1) \times 4$	0.76
	$2.97(11) \times 1$	0.09

		1.56
Site <i>A</i> (between the Bi-O and Cu-O sheets)	$2.56(5) \times 4$	1.14
	$2.74(2) \times 4$	0.70
	$2.91(11) \times 1$	0.11

		1.94

summarized.¹⁴ This must be due to the difference in ionic radius of cations. Similar composition variation due to the ionic radius difference has been reported on $\text{La}_{(1+x)}\text{Ba}_{(2-x)}\text{Cu}_3\text{O}_y$.^{15,16} In the case of La-Ba-Cu-O the smaller La ion substitutes for the Ba ion.

In spite of the deficit of (Sr,Ca) in the samples estimated by the electron-probe microanalysis, we obtained the x-ray diffraction pattern for a highly-*c*-oriented crystal as shown in Fig. 3. The result of the EPMA analysis is subject to some uncertainty. A Weissenberg x-ray diffraction pattern of the samples was reported in Ref. 12. We denote the samples as $\text{Bi}_2(\text{Sr,Ca})_3\text{Cu}_2\text{O}_y$ from these results. Therefore, the interchangeability of Sr and Ca in the lattice sites of the crystal is not specific to the samples used in this investigation. Generally, the substitutional defects are the source of the spectroscopic results in single-crystal samples.

The Bi $4f_{7/2}$ electron binding energy is 158.0 eV as shown in Fig. 4, which is slightly larger than that of Ba-BiO₃ (157.8 eV).¹⁷ The Bi $4f_{7/2}$ electron binding energies for Bi, NaBiO₃, Bi₂O₄·2H₂O, and Bi₂O₃ are 156.8, 158.8, 159.0, and 158.6 eV, respectively.¹⁸ These data may suggest that one should not expect to be able to define the oxidation state of Bi in oxygen coordination in terms of the

core-electron binding energy.

Bond valence sums for Bi in the Bi-O sheet (site *C*) and between the Bi-O and Cu-O sheets (site *A*) were also calculated and are listed in Table II. The value for Bi in site *C* is 1.56, which is smaller than that in site *A* (1.94). This result suggests that the Bi ion located in site *A* possesses larger valence than that in site *C*.

The Bi $4f$ spectrum can be partitioned into two components as shown in Fig. 4. The Bi *L* peak is positioned at 158.0 eV and that of *H* peak is positioned at 159.1 eV. The *L* and *H* peaks can readily be assigned to the Bi ions located in sites *C* and *A*, respectively. The *H* peak intensity corresponds to 13% of the total Bi intensity.

Recently, structure analysis of the $\text{Bi}_2(\text{Sr,Ca})_3\text{Cu}_2\text{O}_{8.2}$ superconducting crystal has been performed.¹⁹ It is based on the computer simulation of a high-resolution transmission electron microscope image. It is reported that 12% of the Bi ions were located in site *A* and the remaining Bi ions occupied site *C*. The result of x-ray photoelectron spectroscopy is consistent with that of computer-simulation structure analysis of transmission electron microscope images. We can readily determine the distribution of Sr, Ca, and Bi in the $\text{Bi}_2(\text{Sr,Ca})_3\text{Cu}_2\text{O}_y$ crystal by x-ray photoelectron spectroscopy contrary to x-ray diffraction and

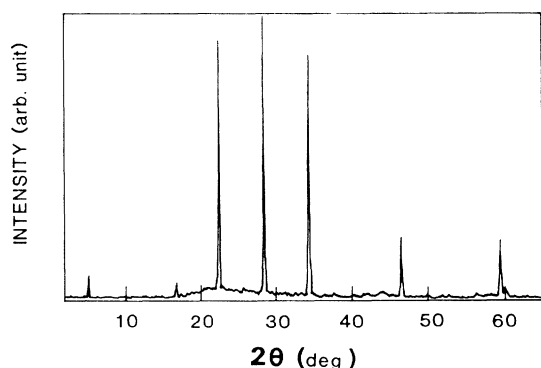


FIG. 3. X-ray diffraction pattern over the 2θ range from 2° to 65° for the single-crystalline Bi-Sr-Ca-Cu-O samples. (002), (006), (008), (0010), (0012), (0016), and (0020) reflections with the Miller indices are clearly observed.

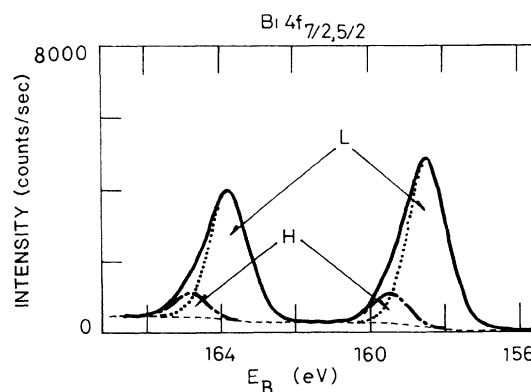


FIG. 4. The Bi $4f$ electron spectrum of the single-crystalline Bi-Sr-Ca-Cu-O samples. The separated peaks have a shape of 100% G and 1.17 eV full width at half maxima. The binding-energy difference between *L* and *H* peaks was 1.1 eV.

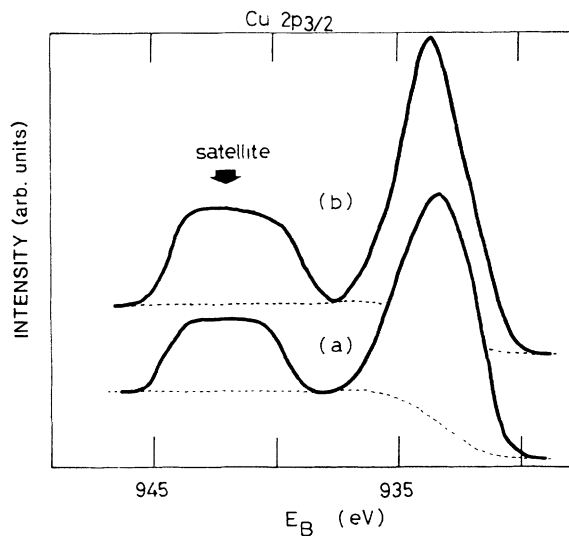


FIG. 5. The Cu $2p_{3/2}$ electron spectrum of the single-crystalline Bi-Sr-Ca-Cu-O samples (a) and that of the $\text{YBa}_2\text{Cu}_3\text{O}_{6.9}$ crystals (b) are combined into one figure to facilitate comparisons. The spectrum (b) was measured with the identical conditions to that of the spectrum (a).

transmission electron microscopy.

The Cu $2p_{3/2}$ electron binding energy is 932.9 eV, which is smaller than that in $\text{YBa}_2\text{Cu}_3\text{O}_{6.9}$ crystal (933.6 eV) (Ref. 20) as shown in Fig. 5. The greater electron binding energy corresponds to the greater valence of Cu in these oxides. Consequently, the mean Cu valence of the Bi-Sr-Ca-Cu-O samples is smaller than that of $\text{YBa}_2\text{Cu}_3\text{O}_{6.9}$ crystal. Moreover, the satellite structure of the spectra due to d^9 electron state²¹ is observed. It confirms the presence of dominantly Cu^{2+} species and the charge transfer between Cu and O atoms in these crystals. The intensity ratio of satellite peak to main peak of the Bi-Sr-Ca-Cu-O samples is 0.40, which is smaller than that of $\text{YBa}_2\text{Cu}_3\text{O}_{6.9}$ (0.56). These features of lower Cu

valence in the Bi-Sr-Ca-Cu-O samples relative to the $\text{YBa}_2\text{Cu}_3\text{O}_{6.9}$ may be due to lack of higher valence Cu presented in the Cu-O chain in $\text{YBa}_2\text{Cu}_3\text{O}_{6.9}$ structure. Dominant charge carriers of the Bi-Sr-Ca-Cu-O crystal are holes¹² which are supplied to the Cu-O plane similarly to the La-Sr-Cu-O and Y-Ba-Cu-O systems. There must be strong Cu d -O p interactions bringing about Cu^{2+} - Cu^{3+} charge fluctuations. The possible resonant coupling to, and enhancement of, the natural ground-state Cu^{2+} - Cu^{3+} fluctuations between in-plane Cu atoms may be important for superconductivity.²² The mean Cu valence variation from the Bi-Sr-Ca-Cu-O to Y-Ba-Cu-O systems may be reflected in their transition temperatures.

IV. CONCLUSION

The present experiment leads to the conclusion that the Sr, Ca, and Bi atoms in the lattice sites of the single-crystalline Bi-Sr-Ca-Cu-O samples are electronically distinguishable as expected on the basis of the $\text{Bi}_2(\text{Sr,Ca})_3\text{Cu}_2\text{O}_y$ crystal structure. We can readily determine the distribution of Sr, Ca, and Bi in the cation sites by x-ray photoelectron spectroscopy contrary to x-ray diffraction and transmission electron microscopy. The mean Cu valence of the Bi-Sr-Ca-Cu-O samples, supposed to $2+$, is lower than that of the $\text{YBa}_2\text{Cu}_3\text{O}_{6.9}$ crystal. These features of electronic state of the Bi-Sr-Ca-Cu-O samples can be explained by the proposed $\text{Bi}_2(\text{Sr,Ca})_3\text{Cu}_2\text{O}_y$ crystal structure. Possibly strong Cu $3d$ -O $2p$ interactions bring about Cu^{2+} - Cu^{3+} charge fluctuations. For obtaining higher-temperature superconductivity (105 K) in the Bi-Sr-Ca-Cu-O system, it may be needed to increase the Cu^{3+} component in the crystal.

ACKNOWLEDGMENTS

The authors thank Dr. B. V. Crist of Hakuto Co., Ltd. for the small-spot ESCA measurement, and Dr. T. Niita, Dr. K. Wasa, and Dr. F. Konishi for support of this work.

*Permanent address: Materials Characterization Department, Matsushita Technoresearch, Inc., Moriguchi, Osaka 570, Japan.

¹J. G. Bednorz and K. A. Müller, *Z. Phys. B* **64**, 189 (1986).

²K. Kishio, K. Kitazawa, S. Kanbe, I. Yasuda, N. Sugii, H. Takagi, S. Uchida, K. Fueki, and S. Tanaka, *Chem. Lett.* 429 (1987).

³R. J. Cava, R. B. van Dover, B. Batlogg, and E. A. Rietman, *Phys. Rev. Lett.* **58**, 408 (1987).

⁴M. K. Wu, J. R. Ashburn, C. J. Torng, P. H. Hor, R. L. Meng, L. Gao, Z. J. Huang, Y. Q. Wang, and C. W. Chu, *Phys. Rev. Lett.* **58**, 908 (1987).

⁵H. Maeda, Y. Tanaka, M. Fukutomi, and T. Asano, *Jpn. J. Appl. Phys.* **27**, L209 (1988).

⁶E. T. Muromachi, Y. Uchida, A. Ono, F. Izumi, M. Onoda, Y. Matsui, K. Kosuda, S. Tanaka, and K. Kato (unpublished).

⁷R. M. Hazen, C. T. Prewitt, R. J. Angel, N. L. Ross, L. W. Finger, C. G. Hadjidakos, D. R. Veblen, P. J. Heaney, P. H.

Hor, R. L. Meng, Y. Y. Sun, Y. Q. Wang, Y. Y. Xue, Z. J. Huang, L. Gao, J. Bechtold, and C. W. Chu (unpublished).

⁸J. M. Tarascon, Y. Lepage, P. Barboux, B. G. Bagley, L. H. Greene, W. R. McKinnon, G. W. Hull, M. Giroud, and D. M. Hwang, *Phys. Rev. B* **37**, 9382 (1988).

⁹M. A. Subramanian, C. C. Torardi, J. C. Calabrese, J. Gopalakrishnan, K. J. Morrissey, T. R. Askew, R. B. Flippen, U. Chowdhry, and A. W. Sleight (unpublished).

¹⁰Y. Matsui, H. Maeda, Y. Tanaka, and S. Horiuchi, *Jpn. J. Appl. Phys.* (to be published).

¹¹Y. Matsui, H. Maeda, Y. Tanaka, and S. Horiuchi, *Jpn. J. Appl. Phys.* **27**, L372 (1988); **27**, L372 (1988).

¹²H. Takagi, H. Eisaki, S. Uchida, A. Maeda, S. Tajima, K. Uchinokura, and S. Tanaka, *Nature* **332**, 236 (1988).

¹³I. D. Brown and D. Altermatt, *Acta Crystallogr. Sect. B* **41**, 244 (1985).

¹⁴A. K. Cheetham, A. M. Chippindale, and S. J. Hibble, *Nature* **333**, 21 (1988).

- ¹⁵I. Nakai, K. Imai, T. Kawashima, and R. Yoshizaki, *Jpn. J. Appl. Phys.* **26**, L1244 (1987).
- ¹⁶E. T. Muromachi, Y. Uchida, A. Fujimori, and K. Kato, *Jpn. J. Appl. Phys.* **26**, L1546 (1987).
- ¹⁷G. K. Wertheim, J. P. Remeika, and D. N. E. Buchanan, *Phys. Rev. B* **26**, 2120 (1982).
- ¹⁸C. D. Wagner, W. M. Riggs, L. E. Davis, J. F. Moulder, and G. E. Muilenberg, in *Handbook of X-ray Photoelectron Spectroscopy* (Perkin-Elmer, Eden Prairie, Minnesota, 1979).
- ¹⁹S. Horiuchi, H. Maeda, Y. Tanaka, and Y. Matsui, *Jpn. J. Appl. Phys.* (to be published).
- ²⁰S. Kohiki, T. Hamada, and T. Wada, *Phys. Rev. B* **36**, 2290 (1987).
- ²¹L. Yin, I. Adler, T. Tsang, L. J. Matienzo, and S. O. Grim, *Chem. Phys. Lett.* **24**, 81 (1974).
- ²²C. L. Fu and A. J. Freeman, *Phys. Rev. B* **35**, 8861 (1987).